Aerodynamics Study of Fixed-Wing MAV: Wind Tunnel and Flight Test

C. Thipyopas and N. Intaratep

Department of Aerospace Engineering, Faculty of Engineering, Kasetsart University
50 Phaholyothin Rd., ChatuChak, Bangkok 10900, Thailand

ABSTRACT

Obtaining accurate aerodynamic characteristics of in-flight Micro Air Vehicles (MAVs) was viewed as difficult, due to the nature of very low Reynolds number, 3D complex flow, and strong influence from propulsion slipstream. This paper presents the study of the tailless, fixed-wing MAV, KuMAV-001, performed at Kasetsart University. The team investigated different analysis and testing methods to determine the aerodynamics characteristics of this MAV. The Vortex Lattice Method was introduced in the conceptual design phase and helped with the evaluation of the 3D effects for winglet configurations. The wind tunnel tests with main wing and fully configured MAV were conducted for powered and unpowered models. The influence of propulsion-induced flows on C_L, C_D, and $C_M(cg)$ was investigated during the wind tunnel testing. Verification of the performance results are to be completed with flight test data in the future.

1 INTRODUCTION

Micro Air Vehicles have been of interest for more than 10 years. Many concepts have been realized and successfully flown for both military and civilian applications. This recent development has been made possible thanks to the progress in miniature size control systems. Originally aimed for outdoor missions, the MAV design in the last few years has also been tested for indoor flights. ISAE-Supaero initially incorporated an indoor mission to the international MAV flight competition in September 2007.

A fixed-wing MAV is suitable for outdoor missions due to its high forward flight efficiency. This was successfully demonstrated by many fixed-wing MAVs, such as the BlackWidow, a flexible wing platform of the University of Florida and the MAVs from the University of Arizona. On the other hand, a rotorcraft MAV provides good hovering and low speed flight required in indoor missions. There have been various unconventional rotorcraft concepts: tri-rotor, quad-rotor, coaxial rotor as well as flapping-wing type MAVs under continuing development. The famous DelFly [1] has outstandingly presented complex aero-structure mechanism for miniature flying vehicles.

Even with these achievements, more investigation and sophisticate test equipments are still necessary for understanding this difficult subject.

Currently, multi-mission capabilities are of great interest. A new rotorcraft design has been studied and developed for a multi-mission UAV [2]. Many rotorcraft MAVs extend their task for outdoor missions and did reasonably well. In the last few years, the rotorcraft concept has won over the fixed-wing configuration in both outdoor and indoor competition. Arguably, this accomplishment may have been the result of the limitation of the competition field size. Hence, the fixed-wing configuration could remain an apt option for outdoor assignments, particularly in high turbulence and unsteady flows [3].

Multi-mission MAVs have also been studied in fixed-wing configurations, particularly at the University of Arizona [4] and at the Institut Superieur de l'Aeronautique et de l'Espace (ISAE-Supaero) [5]. In Thailand, the market survey of UAV applications indicated that a fixed-wing configuration is more fitting to domestic requirements, which include real-time observations of forest, traffic, electrical lines and pipes. The Department of Aerospace Engineering (AE), Kasetsart University (KU) initially started working on a fixed-wing MAV design in 2009 with a primary focus on aerodynamics.

Aerodynamic characteristics are significant to the improvement of MAVs' performance and capacity. At very critically low Reynolds numbers, MAVs' flight efficiency is comparatively poor. Strong three-dimensional flow of extremely low aspect ratio wings introduces more difficulty to the prediction of their aerodynamic characteristics. Furthermore, there are strong flow interactions between propulsion system, wing and airframe. Many studies have been focusing on the effects of propulsion slipstream on the aerodynamics of MAV wings. Longitudinal aerodynamic characteristics affected by propellers have already been extensively investigated [6,7]. Favorable or unfavorable results of the interaction highly depend on the installation angle of the propellers. As displayed in MITE MAV, the strong wingtip vortex of the very low aspect ratio wing is suddenly reduced when a propeller was placed at wingtip. Shkahavey *et al.* [8] empirically predicted thrust requirement for hovering and level flight of their first VTOL MAV by considering additional drag induced by propulsion. In this design, a wing is divided into two parts; the central part submerged in the propeller-induced slipstream and the external part influenced by freestream only.

At present, the numerical methods are not sufficiently reliable to determine accurate aerodynamic coefficients and often require wind tunnel testing for validation. However, there are very few experimental data of low Reynolds number MAVs unlike larger air vehicles. Both force and speed are relatively small and difficult to measure. To obtain correct aerodynamic characteristics, extremely developed facilities, such as those at the University of

---

Florida [9] and the ISAE [10], are necessary. The wind tunnel tests are certainly helpful for the study of low Reynolds number problems as seen in many publications. However, such experimental work has not always yielded results corresponding to real-flight characteristics. The study of Watkins [11] exhibited large variations in the real environment flow where highly turbulent and unstable flow was observed. With no conclusion on the best method to predict aerodynamics characteristics of MAV, the wind tunnel test results then should be compared with other methods. Flight test is one solution used by Ostler [12] to study aerodynamic characteristics of a flying wing in leveled flight. Longitudinal aerodynamic coefficients were calculated from flight data.

The present paper describe methods for obtaining the longitudinal aerodynamic characteristics of the tractor-propulsive fixed-wing KU-MAV001. These methods include a simple Vortex Lattice Method, a small-scale wind tunnel test, a flying-scale wind tunnel test with and without propeller, and a flight test.

2   KUMAV-001: CONCEPTUAL DESIGN AND PROTOTYPE

The team at Kasetsart University started working with a fixed-wing MAV. Due to a lack of experience and research equipments for low Reynolds number aerodynamic testing, the monoplane wing studied by the Arizona State University (ASU) [13] was selected as a baseline model to compare results. The KU design consists of propulsive tractor and elevon configuration as is most often found in MAVs. A relatively larger size wing with a span of 50 cm was selected since local commercial components and experienced pilot were not available for smaller size air vehicle. Estimated mass is around 500 grams. As a result, the model of ASU is scaled up 3 times to obtain a wing span of 45 cm. A fuselage was added to a thick airfoil E212 cross section to allow for practical center of gravity (CG) arrangement. The mission requirement was set with a flight speed of 7 to 15 m/s and minimum endurance of 20 minutes. Finally, the Paparazzi System developed by ENAC team [http://paparazzi.enac.fr/wiki/Main_Page] was chosen for the autopilot version. A summary of design configuration is mentioned in Table 1.

Table 1: KUMAV-001 design configuration

Parameter		Parameter	
Airfoil	E212	Max.Thickness	10.55%c
Root chord	45 cm	Tip chord	39 cm
Aspect ratio	1.07	Span	45 cm
LE Swept	17deg	Dihedral	0 deg
Aerodynamic Center	22% Cr = 10cm LE_r	Center of gravity	7.5% = 7cm LE_r
Control surface	20% LE_r = 9cm	Flight Speed	7-15m/s

The CG location and the size of the control surfaces were achieved using the Vortex Lattice Method. The *Tornado* program [http://www.redhammer.se/tornado/] gave the aerodynamic center at 10cm from the leading edge on the wing root chord (LE_r). The CG position was then marked forward at 7cm (static margin of 7.5%). The control surfaces chord length of 20% of the root chord was selected

to minimize drag at a cruise speed of 10 m/s and with no power.

By this point, all components and their weights were known except for the propulsion system. The propulsion set was estimated from the *Qprop* program [http://web.mit.edu/drela/Public/web/qprop/]. Various on-shelf propellers with diameters of 15.2 to 22.9cm were calculated and compared. The two main design constrains for the propulsion system were being the most efficient at the cruise speed (10m/s) and able to reach maximum speed of 15m/s with a suitable rotational speed. Hovering ability was also considered in the calculation but finally not taken into account. Four best candidates ended up being the APC 6x4, 7x4, 7x5, and 8x4. Their efficiencies were on the order of 0.43-0.55. The thrust results from Qprop were in good agreement with the static test results, but torque was under predicted. Comparison plots are presented in Appendix A.

Finally, an RC version of KuMAV-001 illustrated in Figure 1 was fabricated by hotwire-cut foam. The total weight was 550 grams (including a three cells lipo-battery has capacity of 1300 mAh).

Figure 1: KuMAV-001.

3   MODELS AND EQUIPMENTS

3.1   Models

This section provides detailed descriptions of the two wind tunnel models investigated in this study. Each model has its own studying objectives.
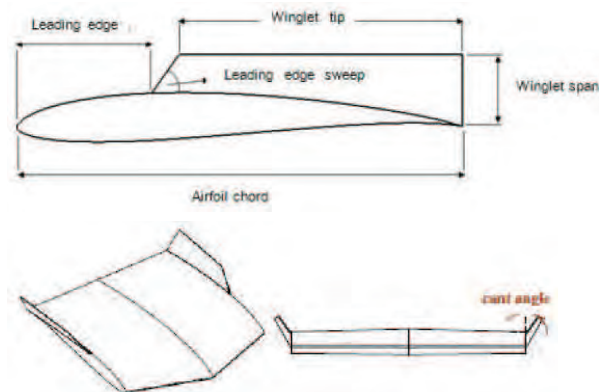

Figure 2: Wind tunnel model for winglet study.

3.1a)   *Half-scale wing model:* This model was designed to study the effect of winglets on wing performance. The lateral characteristics were observed by a 6-components balance. The main wing was made of foam covered by composite material for rigidity. The planform dimensions were half scale of those shown in Table 1. Different winglet parameters, including winglet span, cant angle, leading edge sweep angle, and leading edge location as illustrated in

Figure 2, were designed by the Vortex Lattice Method and evaluated by wind tunnel testing.

3.1b) *Full scale and flying model:* This model was primarily used for flight testing. Longitudinal characteristics were determined by wind tunnel testing using a 3-component balance and were then compared to flight data. The model is the same one as presented in Figure 1 of section 2.

3.2 Force Measurement Systems (for Wind Tunnel Test)

As described in section 3.1, there were two force balance setups used in this study: one for the half-scale model and one for the full-scale model. Both force balance were not designed for very low Reynolds number testing, yet they were the only equipment available in the Department.

3.2a) *6-component balance:* The lateral effects of winglets were of primary interest for this study. The aerodynamic characteristics of the half-scale model were measured using a balance equipped with an ATI 6-component Force/Torque sensor (DALTA model) at its base, as illustrated in Figure 3. The measurement ranges were ±330N for axial and side force with ±990N for normal force. The moment capacity was ±30Nm. The balance was installed on a turn table under the test section so as to vary the yaw angle.

A two-strut mounting system was used to provide support for the model as well as a mechanism for changing the angle of attack. The model weight was carefully observed and subtracted from the test results.
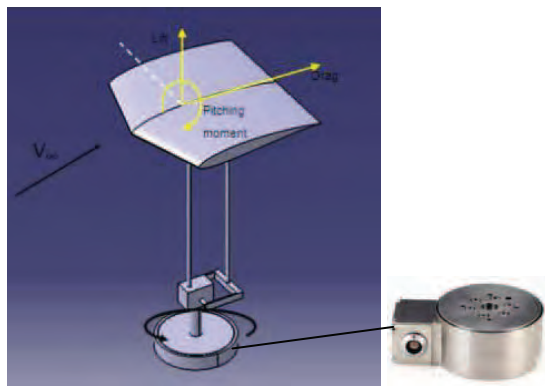

Figure 3: 6-component balance and set up of the half-scale model.

3.2b) *3-component balance:* To simulate level flight conditions, the flying model was supported by a single strut at the CG position. This location was selected to minimize any additional error arising from the force-moment translation. Lift, drag, and pitching moment were obtained directly by a pyramid balance outside the test section. The balance and angle of attack adjustment system using the turn table are shown in Figure 4. The maximum capacities were ±500N and ±50 Nm for force and moment respectively. The accuracies of the balance were 1N and 0.5Nm.

3.3 Closed-Loop Wind Tunnel

Kasetsart closed-loop wind tunnel has a test section of 1m×1m×3m (W×H×L). A contraction ratio of 4 results the maximum speed of 60 m/s generated by a 2m-diameter fan with maximum power consumption of 75kW. The highest speed presented in this study was only 15m/s. The layout of the wind tunnel is displayed in Appendix B. The current equipment of the facility did not allow for measurements of the turbulence intensity. Wind speed was measured by a Pitot-static tube installed in front of the model and a digital manometer with an accuracy of 5Pa.
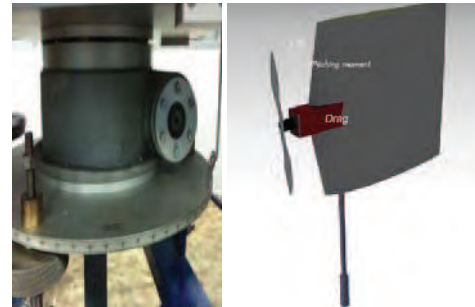

Figure 4: 3-component balance and test set up of the full-scale model.

3.4 Propulsive Measurement

Due to the uncertainties in the results obtained from *Qprop*, the propulsion sets were tested for both static and dynamic performances. An in-house propulsive test bench, using 6N-load cell, was designed to measure thrust and torque. Future improvements of the test bench will include the measurement of other force and moment components will for characterizing propeller performance at various angles of attack. The schematic of the test bench and equipments are presented in Figure 5. The set up included a DC power supply of 30A and 15V max capacity, RC commercial brushless motor speed counter, RC transmitter, digital volt meters, and a National Instruments NI A/D 24 bits converter. The motor was rated at 11.5Vand powered by three battery packs. The measurement parameters included the speed of the propeller (RPM), current (Amp), voltage (Volt), torque (N.m), and thrust (N). Thrust and torque were obtained by averaging 500 samples measured at 500Hz.
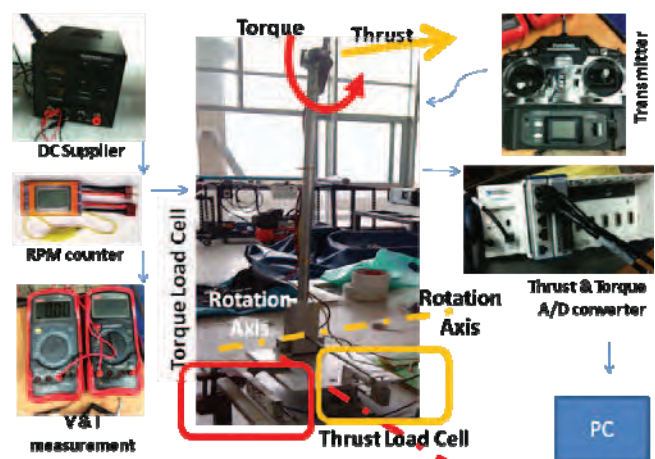

Figure 5: Propulsive Measurement System.

4 METHODOLOGY

4.1 Preliminary Calculation by Vortex Lattice Method

The preliminary estimations of the aerodynamic characteristics for the KuMAV-001 were obtained from the Tornado code. Although the code was not designed for very

low Re flow, the results were acceptable for conceptual design of aerodynamic center, control surface efficiency, and other aerodynamic derivatives at small angle of attacks. The results of these estimations were used for the design of the first prototype mentioned in the section 2.

The code was also used to study the effects of winglets. It gave the preliminary analysis of the winglet configurations, illustrated in Figure 2, used to minimize the number of wind tunnel models.

4.2   Wind Tunnel Test Low Reynolds Number Wing

After successfully obtaining the prototype design from the Vortex lattice Method, the half-scale wing model was tested in the wind tunnel to characterize the effects of winglets on the main wing longitudinal and lateral behaviors. Three winglet models detailed in Table 2 were studied.

The first winglet model was based on the characteristics designed and simulated by ASU. Another two winglet models were selected from Tornado's results. The 2nd winglet model (s60_c60) gave the highest maximum lift-to-drag ratio (L/D) while the 3rd winglet model (s60_c30) had the best lateral stability. The wing model with the winglet s60_c60 is presented in Figure 6.

Table 2: Half Scale Test Model.

Winglet shape	Model			
	No Winglet	8B	S60_c60	S60_c30
Airfoil	-	Flat plate	Flat plate	Flat plate
LE-Swept angle	-	26.6 deg	60 deg	60 deg
LE-Location	-	25.2% c	25.2% c	25.2% c
Span	-	16.9% c	16.9% c	16.9% c
Cant angle (from vertical)	-	0 deg	60 deg	30 deg

Figure 6: Half Scale wing model with winglet s60_c60.

4.3   KuMAV-001RC's Flight Test

As previously mentionned in section 2, the first RC-prototype of the KuMAV001 was build and tested. The first flight was performed with the APC8x6 propeller. Due to limited experience in flying a very low aspect ratio wing model, the flight test did not initially achieve all the objectives. The torque from the propeller was too high for our pilot to control. Winglets were consequently added the damp the rolling motion. The winglets had a 10cm span with a length of 30cm.

The second attempt completed with an endurance of 10 minutes. The third flight was tested by changing the propeller to the APC7x4 model without winglet. This model flew but unstable roll was still an issue.

The addition of the smaller winglets to the same APC7x4

propeller resulted in the first fully successful flight of the KuMAV-001RC .

4.4   Finding Propulsive Characteristics

To evaluate the propulsion performances, the static and dynamic thrusts of a set of propellers (APC8x4, APC7x5, APC7x4 and APC6x4) were measured using the propulsive test bench mentioned in section 3.4.

Thrust and torque of motor-propeller were recorded at different motor speeds, controlled by a radio transmitter sending the PWM signal to the propulsive system. Other parameters measured included motor speed, voltage and current.

Dynamic thrust of selected propeller was also investigated in the wind tunnel at the freestream, velocities of 5, 7.5, and 14.5 m/s. Although propulsive characteristics would change when a propeller was at incidence [14], the current set up has only been studied at zero degree AoA (the propeller disc was normal to freestream flow). The impact of the propeller incidence should be small as long as the angle of attack is less than 20 degrees. The picture of the dynamic thrust test bench used in the wind tunnel is illustrated in Figure 7a.
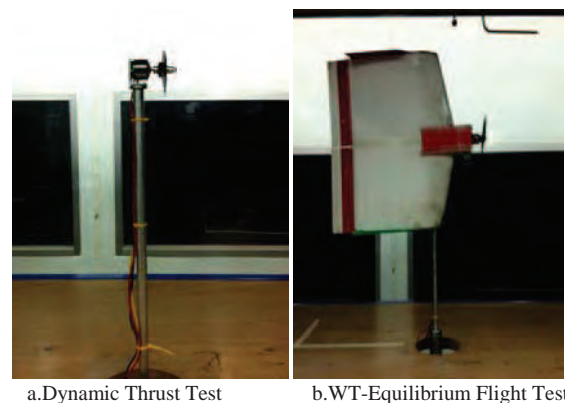

a.Dynamic Thrust Test   b.WT-Equilibrium Flight Test

Figure 7: Wind tunnel test of propeller and full scale model

4.5   Equilibrium Test of Powered MAV: Wind Tunnel

Due to the difficulty and low accuracy of the measurement system for the in-flight test, a wind tunnel experiment was conducted at wind speeds of 5, 7.5, and 14.5 m/s to validate the results. The wind tunnel tests were performed with the real flight RC-model equipped with the APC7x4 propeller as presented in Fig. 7b. Both configurations (the models with and without winglets) were investigated. The equilibrium points (or trim point) for level flight were run at the same wind speeds of 5, 7.5, and 14.5m/s. The throttle, AoA, and elevon setting were adjusted in order to reach zero pitching moment and minimum drag at a fixed wind speed.

The drag correction from the strut effects was performed in real time during the measurements. One of the advantages of the wind tunnel tests is that they generated several data points for different lift configuration while for the flight test, the weight of the model was rather constant or hardly modified (primarily by changing the battery size). In this test, the lift forces of 300g to 500g were produced in the wind tunnel. All necessary parameters were collected including lift, motor speed, motor electrical data, AoA, and approximated elevon deflection angle.

4.6 Traditional Wind Tunnel Test on Unpowered MAV

The wind tunnel testing of the unpowered full-scale model was carried out at the same speeds of 5, 7.5, and 14.5 m/s. At each wind speed, a full polar curve with AoA between 0 and 36deg were produced. Also, the effects of the control surfaces on the aerodynamic characteristics were carefully observed at full deflection using an RC transmitter control.

4.7 Equilibrium Test of Powered MAV: In-Flight

The second flight model was fabricated with the same material and method as the RC model. At this point, the test-flight is scheduled to include a Paparazzi system (PZ), with the normal TWOG system. Due to some shipping delay for the PZ system, the test-flight phase is still in progress. However, the PZ system was successfully tested inside a 1m-span conventional airplane model as illustrated in Figure 8.

The procedure consists in flying the KuMAV-001AT at constant level through two points A and B separated by a distance of 500m and observing the data during the flight. At each speed, 10 flights are performed and results are consequently averaged to determine the longitudinal aerodynamic characteristics. Now that the PZ system has been validated, the flight test is expected to be completed soon.
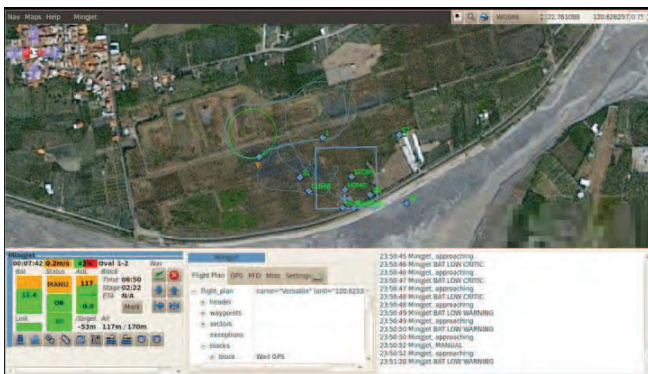
Figure 8: Flight trajectory of Paparazzi system done by conventional plane.

4.8 Result and Data Correction

Two corrections were required for the wind tunnel test data. The first one was a wind tunnel correction due to wall effect. The standard blockage and wall correction of Barlow et al. [15] was applied to the primary data, with a particular focus on the change in AoA. For the equilibrium test in the wind tunnel, the propulsive force or thrust (T) was subtracted out to determine the exact wing aerodynamic characteristics. The equilibrium level flight is detailed in Equations 1-3 from which the C_L, C_D, and C_M of MAV can be calculated.

$$(1) \qquad \sum F_x = 0: \ Tcos(\alpha) + D = 0$$

$$(2) \qquad \sum F_z = 0: \ Tsin(\alpha) + L + mg = 0$$

$$(3) \qquad \sum M_y = 0: \ Tz + M_{cg} = 0$$

In Eq. (1-3), L, D, M, m, g and α are respectively the lift, drag, pitching moment, mass, gravitational acceleration and AoA,. Since the thrust vector was aligned with the wing chord line, the distance z is equal to zero.

5 RESULTS AND COMPARISON

5.1 Comparison with ASU model

The lift coefficients for the half-scale model without winglet are comparable to the numerical values produced by ASU (Figure 9). Both results have similar lift-curve slopes. The wind tunnel results appear to have some non-linearity in the lift curve slope possibly due to some uncertainty in the angle of attack.
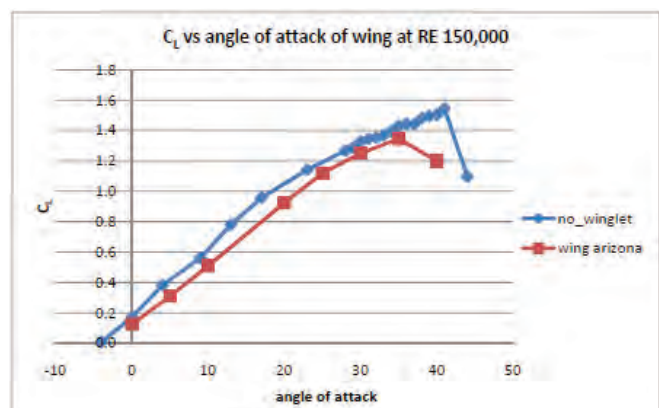
Figure 9: Comparison of CFD and Wind Tunnel Test.

5.2 Effect of winglet

The effects of the winglets on the half-scale model performance and stability were studied in the wind tunnel at Reynolds numbers between 150,000 and 250,000. Longitudinal static stability does not appear to be influenced by the winglets. Figure 10 shows however that the static lateral stability is clearly affected. The most stable model is the 8B model due to its cant angle of 0 deg and to the fact that the vertical projection of the winglet area behind the aerodynamic center is greater than for other models.
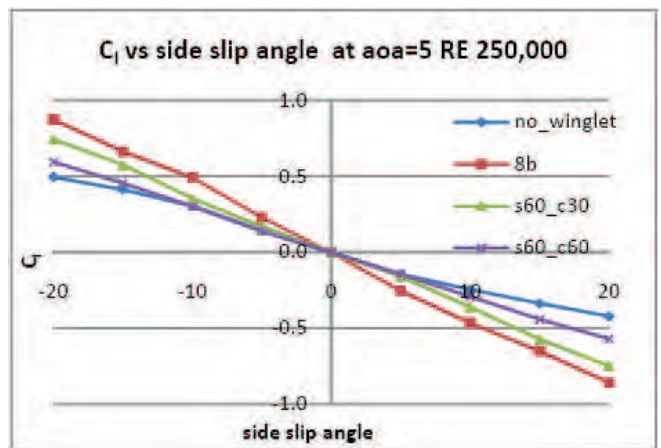
Figure 10: Effect of winglet on lateral static stability.

Winglets also have a strong effect on L/D. They are usually found to increase the lift curve slope and drag. Considering the L/D plot shown in Figure 11, the winglets do not appear to improve the wing aerodynamic performance. On the contrary, they seem to reduce the L/D of the MAV wing.
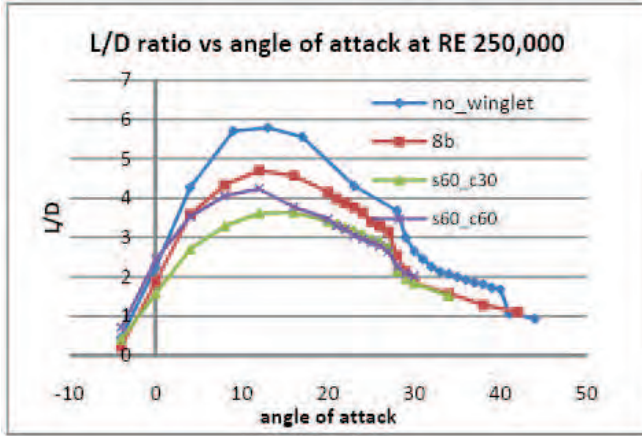

Figure 11: Effect of winglet on L/D.

5.3   Thrust results

Propulsive force measured by load cell is presented in Figures 12 and 13. Thrust is plotted against the electric input power consumption in order to determine the most efficient propulsive system. The APC 6x4 and 7x4 propellers produce the best efficiencies. Comparison between these two propellers reveals that the APC 7x4 is able to provide higher maximum thrust. Since this propeller has also already been tested in the RC flight test, it was selected for the next step of the project.
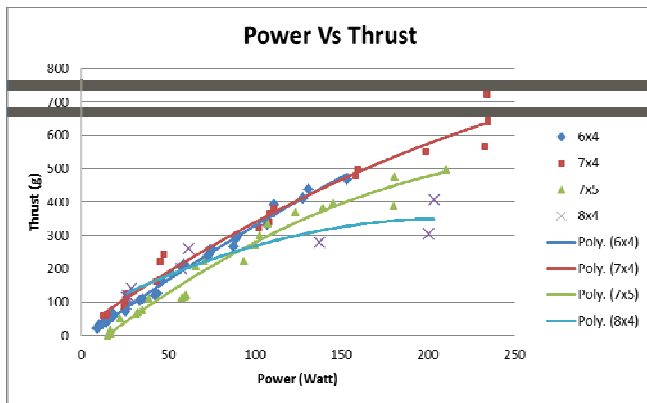

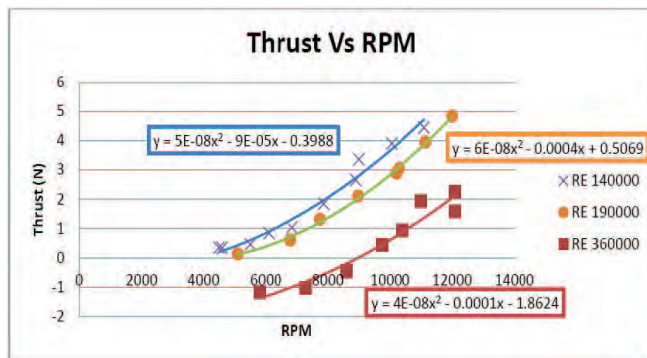Figure 12: Static Thrust of Propeller APCs.

Figure 13: Dynamic Thrust of Propeller APC 7x4

The dynamic thrust results are used in the thrust prediction of the powered MAV model. Dynamic thrusts for the APC 7x4 propeller at wind speeds of 5.5, 7.5, and 14.5 m/s are plotted as a function of propeller speed. In Figure 13, dynamic thrust is plotted for Reynolds numbers of 140000, 190000, and 360000, corresponding to the speeds of 5.5, 7.5, and 14.5m/s respectively. The data was fitted with polynomial functions to extract the variation of the dynamic thrust with propeller speed. Such analysis were also performed as function of the input current but is not presented here. It will be however used to present with the flight test results.

5.4   Full Scale Result

This project also plans to test full-scale flight model in both by wind tunnel and free flight environments. Due to some delay in obtaining the flight control system, the data presented in the current study pertains only to the wind tunnel test. The flight test results will be published at a later date.
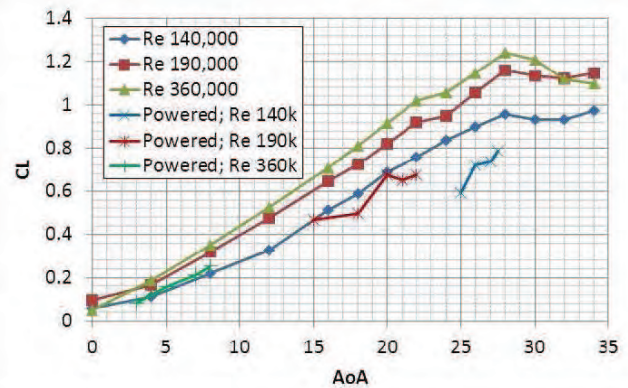

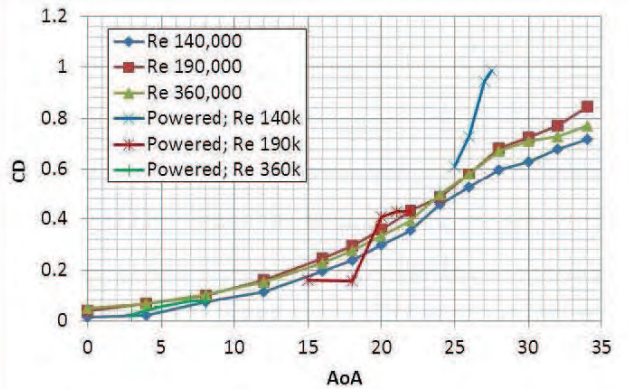Figure 14: Lift Coefficient of Full Scale Model.

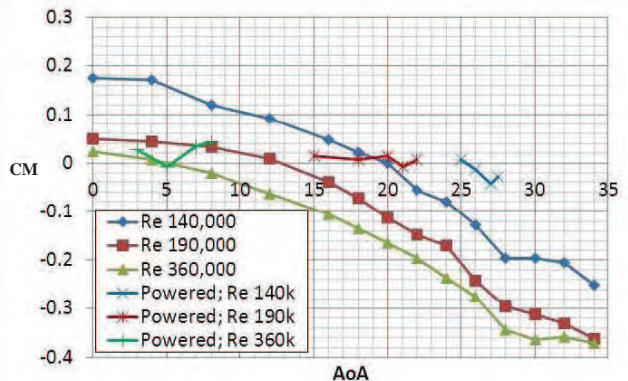Figure 15: Drag Coefficient of Full Scale Model.

Figure 16: Pitching Moment Coefficient at C.G. of Full Scale Model.

The results for lift, drag, and pitching moment of the model without winglets are presented in Figures 14-16. C_L, C_D and $C_M(cg)$ of powered and unpowered models are computed and plotted. Firstly, the Reynolds number effects are clearly revealed by the results of unpowered model as the lift curve slope increases with Re. Stall angle is consistently at about 28 degrees. Comparing the lift coefficient of the powered and unpowered models at high Re and low AoA shows that the C_L of the powered model is slightly lower than that of the unpowered model. The difference increases with decreasing Re and increasing AoA. These results clearly highlight the effects of propulsive induced flow on the main wing aerodynamic characteristics.
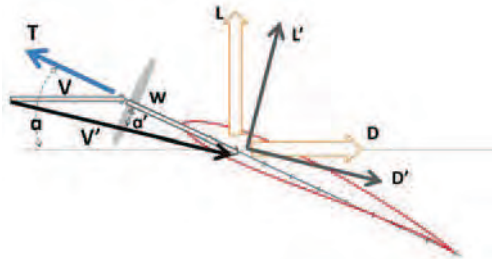

Figure 17: Schematic of Propulsive Induced Flow Vector.

Following the nomenclature presented in Figure 17 [16], an MAV is assumed to be flying from right to left with a speed V and at the AoA of α deg. Without propeller, lift and drag are represented by the thick orange arrows. When the propeller is introduced, thrust T is then produced (tractor propeller in this configuration). According to momentum theory, induced velocity w is obtained by Equation 4.

$$（4）\qquad w = \sqrt{[(2T)/(\rho A)] + [V\, cos(a)]^2}$$

Therefore, the resultant velocity vector acting on the main wing is V' and the local AoA is α' as illustrated. There are 2 main effects of propulsive-induced flow which directly impact the aerodynamic characteristics: the reduction of local AoA (from α to α') and the increase of the local speed (from V to V') resulting in the modified local lift and drag L' and D' respectively. Finally, the lift and drag force on the MAV must be a projection vector product of L' and D' to $(X$ and $Y)$, the freestream aerodynamic axes with an angle of $(\alpha-\alpha')$. The larger local velocity enhances the aerodynamic coefficients while the reduction of the local AoA degrades them. However, according to Figure 14, C_Ls decreased due to the effects of propulsive-induced flow as a result of the reduction in the local AoA rather than the increase of the local velocity.

Drag coefficient results shown in Figure 15 have no clear tendency except at the lowest Re. For high Re, the C_D of the powered model is just slightly less than that found in the unpowered model, but it is higher at the lowest Re. At the high speed, the enhanced velocity behind the propeller is negligible compared to that at low speed. Therefore it appears that the increment of drag force from induced speed is low.

Consider now a regular curve of C_D vs AoA. C_D changes very little at very low AoA (parabola curve). Thus, the reduction of local AoA induced by the propeller does not present in the C_D curves. On the other hand, at high AoA and low flight speed, the propeller flow strongly affects C_D on both AOA and local velocity account which may compensate each other. However, the sum of drag also includes the component of L' as the local AoA changes. Consequently, additional ('propulsive' induced) drag is presented on the model. The net effect is the same for the pitching moment presented in Figure 16. Hence, more accurate measurements of the force and local flow speed behind the propeller are necessary to obtain a clear picture of the flow behavior at each flight speed. Hopefully, the flight test results will provide an insight and confirm the wind tunnel data.

6 CONCLUSIONS

This paper presents the development of Micro Air Vehicles (MAVs) at the Department of Aerospace Engineering, the Faculty of Engineering, Kasetsart University, Bangkok, Thailand. The 45cm-span fixed-wing MAV named KuMAV-001 was designed and studied. The wing model was based on the study of the Arizona State University (ASU).

Aerodynamic characteristics of KuMAV-001 were investigated through several methods including an estimation by the Vortex Lattice Method from *Tornado* code, half-scale and full-scale wind tunnel tests, powered model wind tunnel tests, and data from flight test.

New experimental facility was designed and constructed to examine the propulsive characteristics. The *Qprop* code was used to validate the measurements. Dynamic thrust of various propellers was also measured in a 1m×1m test section wind tunnel. The effects of different winglets were evaluated by half-scale wind tunnel testing using 6-component force balance to evaluate lateral characteristics as well as longitudinal characteristics. The results were then compared with that provided by ASU.

A full scale model was fabricated and tested in both free flight and in a wind tunnel. In the wind tunnel test, the measurement for the full scale model was performed using a 3-component longitudinal force balance. The test was conducted to simulate level flight conditions; pitching moment = 0 and result drag force = 0. An unpowered model was also built and tested for conventional aerodynamic data.

Due to the propulsive induced flow effects on the central part of model, local angle of attack and velocity were modified. This phenomenon explains the difference in the longitudinal aerodynamic characteristics between powered and unpowered models. A method by McCormick on the propulsive induced effects was offered as an explanation for the difference between the wind tunnel results of powered and unpowered models. However some of this difference may also be the result of errors introduced by the accuracy of facility and measurement system.

7 ON-GOING EFFORTS

MAV activity is just starting at Kasetsart University. But the success of the current study highly motivates team members and students. Students suddenly got an opportunity to apply what they had learned from their classes while discovering an entertaining new field. The

MAV study is continuing since it is very attractive and a field of great potential in Thailand.

The work is now focused on the development of new multi-mission platforms aimed at using new MAV in forest and city environment. VTOL and low speed flight capacity are very necessary for such areas. New propulsion system with better capabilities for forward and hovering flights will be researched as well as the study on optimizing propeller-wing interaction. Active morphing wing with propulsive interaction will be another interesting option to improve flight performance. A new sensor for non-GPS environment will be studied as inter-departmental research projects. The Department of Aerospace Engineering at Kasetsart University will welcome any cooperation in MAV research and education.

ACKNOWLEDGMENT

REFERENCES

[1] G. Mark, B. Bart, R. Bart, R. Rick, O. Bas van, and B. Hester, "Improving flight performance of the flapping wing MAV DelFly II", Proceedings of IMAV 2010, Braunschweig, Germany, July 6-9, 2010.

[2] G. Grondin, C.Thipyopas, and J.M. Moschetta, "Aerodynamic Analysis of a Multi-Mission Short Shrouded Coaxial UAV: Part III – CFD for Hovering Flight", 28th AIAA Applied Aerodynamics Conference, Chicago, Illinios, June 28-1, 2010.

[3] M. Abdulrahim, S. Watkins, R. Segal, M. Marino, J. Sheridan, "Dynamic Sensitivity to Atmospheric Turbulence of Unmanned Air Vehicles with Verying Configuration," Journal of Aircraft 2010, Vol. 47, no. 6, p. 1873-1883.

[4] J.M. Moschetta, B.Bataillé, C. Thipyopas, and S. Shkarayev, "On-Fixed-Wing Micro Air Vehicles with Hovering Capacities", 46th AIAA Aerospace Sciences Meeting and Exhibit, Reno, Navada, Jan 7-10, 2008.

[5] R.Carr, J.M. Moschetta, G. Mehta, and C. Thipyopas, "A Tilt-Body Fixed-Wing Micro Air Vehicle for Autonomous Transition Flight," Proceedings of IMAV 2010, Braunschweig, Germany, July 6-9, 2010.

[6] C. Thipyopas and J.M. Moschetta, "A Fixed-Wing Biplane Micro Air Vehicle for Low Speed Missions," International Journal of Micro Air Vehicles, Vol.1, p. 33.

[7] W. Null, A. Noscek and S. Shkarayev, "Effects of Propulsive-Induced Flow on the Aerodynamics of Micro Air Vehicles," 23rd AIAA Applied Aerodynamics Conference, Toronto, June 6-9, 2005.

[8] S. Shkarayev, J.-M. Moschetta, and B.Bataillé, "Aerodynamic Design of Micro Air Vehicles for Vertical Flight", Journal of Aircraft, 2008, Vol. 45, no.5, p. 1715-1724.

[9] R. Albertani et al., "Validation of a Low Reynolds Number Aerodynamic Characterization Facilities", 47th AIAA Aerospace Sciences Meeting including the New Horizons Forum and Aerospace Exposition, Orlando, Florida, Jan 5-8, 2009.

[10] Documentaion of Sarb Wind Tunnel, internal report, ISAE, Toulouse, France

[11] S. Watkins, M.Abdulrahim, M.Marino, and S. Ravi, "Flight Testing of a Fixed Wing MAV in Turbulence with Open and Closed Loop Control," Proceedings of IMAV 2010, Braunschweig, Germany, July 6-9, 2010.

[12] J.N. Ostler, "Flight Testing Small, Electric Powered Unmanned Aerial Vehicles," Master thesis, Brigham Young University, 2002.

[13] J. Monttinen, "On the Performance of Micro-Aerial-Vehicles," Mechanical and Aerospace Engineering Thesis, Arizona State University, 2003.

[14] D. Gomez Ariza and J.M. Moschetta, "The Lateral Force Effect on Rotors at Incidence: Application to a Coaxial Rotor Mini-UAV Tail Sitter," 46th Symposium of Applied Aerodynamics, Orleans, France, March 2011.

[15] J.B. Barlow, W.H. Rae, and A. Pope, "Low-Speed Wind Tunnel Testing," Wiley 1999, ISBN0471557749.

[16] B.W. McCormick, Aerodynamics of V/STOL Flight," Dover Publications, INC, 1999, chapter 8.

APPENDIX A: WIND TUNNEL SCHEMATIC
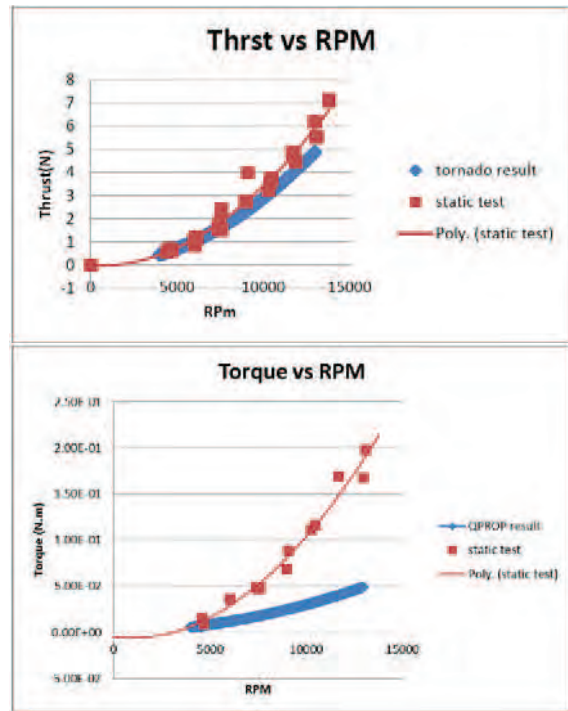
APC 6x4: Result of *Qprop* is compared with the experimental test result. *Qprop* well predict static thrust but it is not good for calculate the torque of motor-propeller.
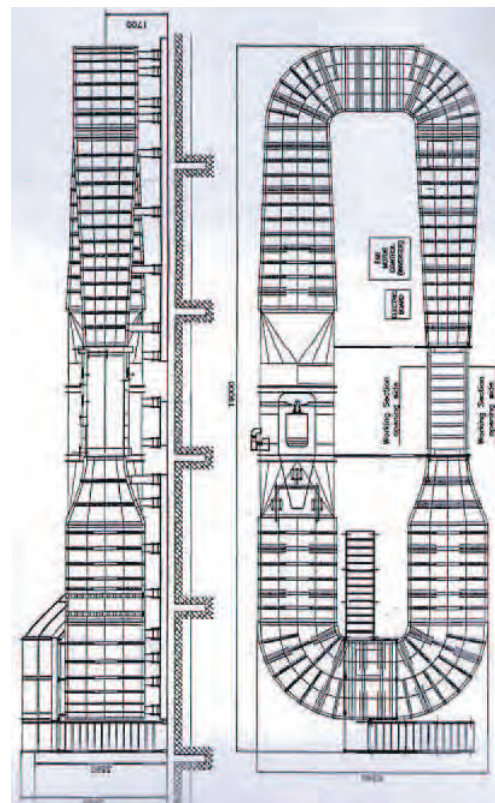
APPENDIX B: WIND TUNNEL SCHEMATIC

Figure A: Closed-loop low speed wind tunnel of Department of Aerospace Engineering, Kasetsart University at Sriracha Campus.